Engagement of $S1P_1$-degradative mechanisms leads to vascular leak in mice

Myat Lin Oo,[1] Sung-Hee Chang,[1] Shobha Thangada,[2] Ming-Tao Wu,[2] Karim Rezaul,[2] Victoria Blaho,[1] Sun-Il Hwang,[3] David K. Han,[2] and Timothy Hla[1]

[1]Center for Vascular Biology, Department of Pathology and Laboratory Medicine, Weill Cornell Medical College, Cornell University, New York, New York, USA.
[2]Center for Vascular Biology, University of Connecticut Health Center, Farmington, Connecticut, USA.
[3]Mass Spectrometry Core Facility, Cannon Research Center, Carolinas Medical Center, Charlotte, North Carolina, USA.

GPCR inhibitors are highly prevalent in modern therapeutics. However, interference with complex GPCR regulatory mechanisms leads to both therapeutic efficacy and adverse effects. Recently, the sphingosine-1-phosphate (S1P) receptor inhibitor FTY720 (also known as Fingolimod), which induces lymphopenia and prevents neuroinflammation, was adopted as a disease-modifying therapeutic in multiple sclerosis. Although highly efficacious, dose-dependent increases in adverse events have tempered its utility. We show here that FTY720P induces phosphorylation of the C-terminal domain of S1P receptor 1 ($S1P_1$) at multiple sites, resulting in GPCR internalization, polyubiquitinylation, and degradation. We also identified the ubiquitin E3 ligase WWP2 in the GPCR complex and demonstrated its requirement in FTY720-induced receptor degradation. GPCR degradation was not essential for the induction of lymphopenia, but was critical for pulmonary vascular leak in vivo. Prevention of receptor phosphorylation, internalization, and degradation inhibited vascular leak, which suggests that discrete mechanisms of S1P receptor regulation are responsible for the efficacy and adverse events associated with this class of therapeutics.

Introduction

Sphingosine-1-phosphate (S1P) is a lipid mediator that interacts with GPCRs to induce cellular responses (1, 2). In mammals, S1P is enriched in plasma and is low in interstitial fluids, thus forming a gradient between vascular and nonvascular compartments. Hematopoietic cells use this S1P gradient as a spatial cue to egress from a low-S1P environment (i.e., lymph nodes, thymus, and peripheral tissues) to a high-S1P environment (i.e., lymph and plasma) (3, 4). The prototypic S1P receptor 1 ($S1P_1$), originally isolated from vascular ECs (5), is essential for the process of lymphocyte egress (6). Recent work suggests that plasma membrane–localized $S1P_1$ on immune cells is essential for efficient egress (7). In addition, complex regulatory mechanisms, including receptor phosphorylation (8), endocytosis, recycling (9), and direct binding with regulatory proteins such as CD69 (10, 11), are involved in the control of plasma membrane residency of $S1P_1$ and lymphocyte egress.

The S1P receptor modulator FTY720, which is phosphorylated by sphingosine kinase–2 (12, 13), interacts with $S1P_1$ at high affinity and activates the receptor (14, 15). However, FTY720P (a phosphorylated derivative of FTY720) potently induces receptor internalization and blocks recycling, resulting in irreversible internalization of $S1P_1$ in vitro (16) and in vivo (7, 17). Thus, FTY720P makes immune cells refractory to the S1P concentration gradient and thereby inhibits egress. However, $S1P_1$ is expressed by other cells, for example ECs, and FTY720P is known to influence the function of these cells (13). Recently, we showed that FTY720P induces polyubiquitinylation of $S1P_1$ and proteasomal degradation in ECs and HEK293 cells in vitro (8). Whether this occurs in vivo is not known. Indeed, plasma S1P is essential for the maintenance of normal barrier function of the vascular endothelium and to resist inflammation-induced vascular leak (18). Additionally, chronic FTY720 treatment in mice inhibits tumor angiogenesis (19).

Clinical studies have demonstrated that FTY720 is highly efficacious in the treatment of multiple sclerosis (20, 21). In phase III studies, oral administration of 0.5–1.25 mg/d FTY720 reduced disease progression better than placebo or β-interferon. However, there was a dose-dependent increase in adverse events, including reduced pulmonary function and increased macula edema. The mechanisms involved in such adverse effects are not known. Since the primary target of FTY720 is thought to be functional antagonism of $S1P_1$ in autoreactive immune cells that induce CNS inflammation and destroy myelinated axons (22, 23), it is important to further define the molecular mechanisms involved in the interaction of FTY720P with $S1P_1$ in various cell types.

In this report, we describe the detailed mechanism of regulation of $S1P_1$ upon binding to FTY720P. We showed that phosphorylation led to multisite polyubiquitinylation of the C-terminal domain that required the E3 ubiquitin ligase WWP2. Moreover, we showed that $S1P_1$ degradation contributed to pulmonary vascular leak in vivo, which suggests that interference with $S1P_1$ levels may lead to vascular pathologies.

Results

FTY720P induces posttranslational modifications in the C-terminal tail of $S1P_1$. To define the posttranslational modifications that occur on $S1P_1$ after FTY720P binding, we developed a robust system to isolate preparative amounts of $S1P_1$. We isolated a stable HEK293 clone expressing the tandem-affinity purification–tagged (TAP-tagged) construct ($S1P_1$-Tap-Tag). Figure 1A illustrates the fusion protein; this construct allowed enrichment of $S1P_1$ by TAP using chitin- and calmodulin-affinity matrices (24). As shown in Figure 1B, efficient purification and elution of $S1P_1$-Tap-Tag fusion protein were obtained, as determined by

Conflict of interest: T. Hla served as a consultant for Connecticut Children's Medical Center, Sidley Austin LLP, and Wilmer Hale LLP.

Citation for this article: *J Clin Invest.* 2011;121(6):2290–2300. doi:10.1172/JCI45403.

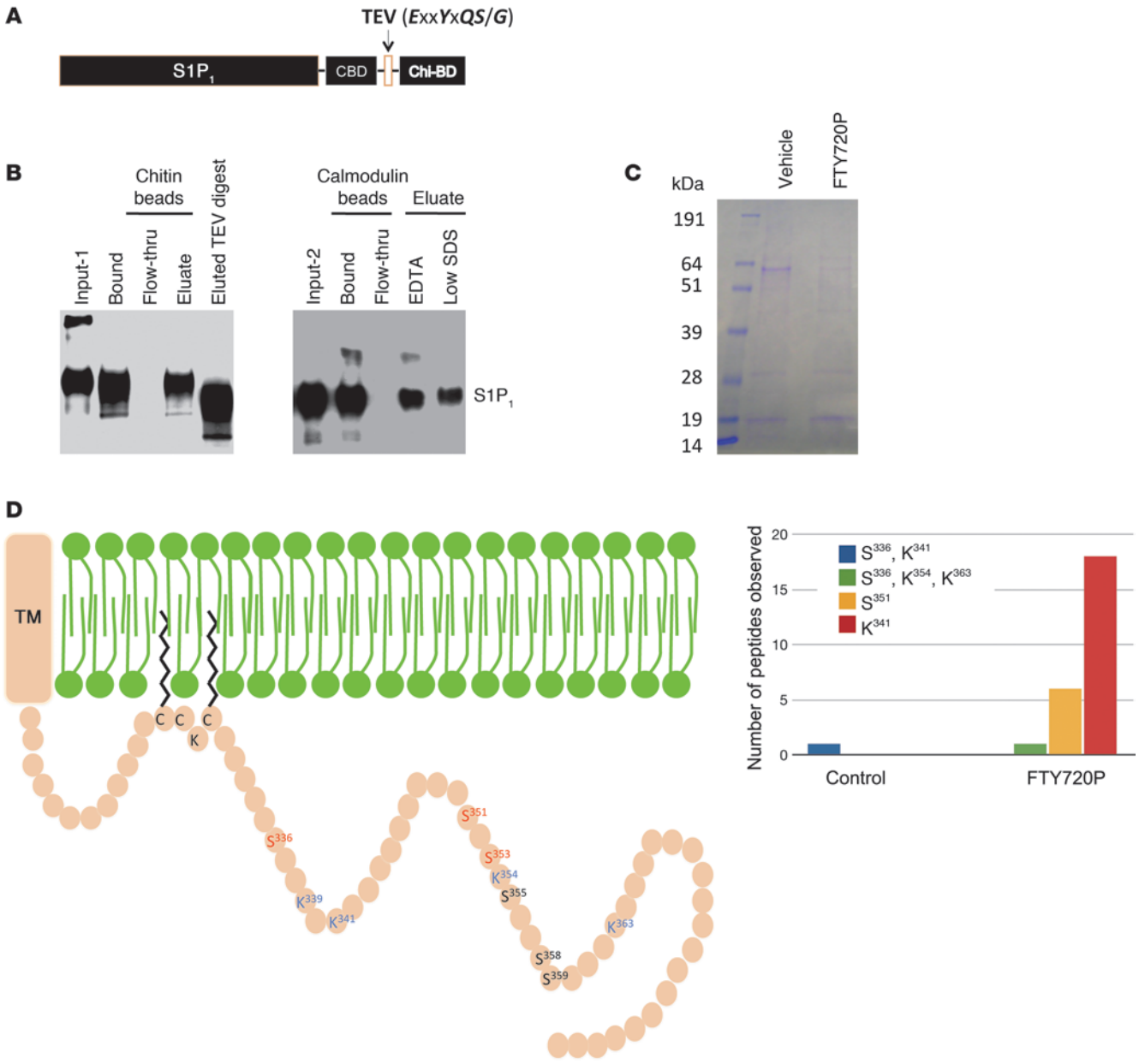

Figure 1

Posttranslational modification of $S1P_1$ after FTY720P treatment. (**A**) Schematic of $S1P_1$ fused with the tandem-affinity construct. CBD, calmodulin-binding domain; Chi-BD, chitin-binding domain. (**B**) Purification and IB analysis of the $S1P_1$ tandem-affinity construct. (**C**) Coomassie blue staining of purified $S1P_1$ from HEK293 cells after treatment with vehicle or FTY720P (100 nM for 30 minutes). (**D**) Schematic diagram of seventh transmembrane domain (TM) and C-terminal tail of $S1P_1$. Shown are the S-palmitoylation sites on cysteine residues (C) as well as phosphorylated serine and ubiquitinylated lysine residues identified by LC/MS/MS. Spectral counts of modified peptides are also shown.

IB analysis. Preparative amounts of $S1P_1$-Tap-Tag fusion protein were isolated from HEK293 cells treated or not with FTY720P for 30 minutes. The resulting eluates were separated by SDS-PAGE (Figure 1C) and stained with Coomassie blue, the gel region between 39 and 85 kDa was cut and trypsin-digested in the gel, and the resultant peptides were analyzed by liquid chromatography–tandem mass spectrometry (LC/MS/MS). The full-length $S1P_1$-Tap-Tag protein was reduced in the FTY720P-treated lane, consistent with the fact that this reagent induces receptor degradation. We identified numerous C-terminal peptides with phosphorylated and ubiquitinylated residues (Table 1). For example, phosphorylation of S^{336}, S^{351}, and S^{353} and ubiquitinylation at K^{341}, K^{354}, and K^{363} were observed. Spectral count analysis indicated a general increase in phosphorylation and ubiquitinylation of C-terminal tail after FTY720P treatment (Figure 1D). Although our LC/MS/MS analysis may not be comprehensive, given the intrinsic difficulty in proteomic analysis of hydrophobic GPCRs, these data nevertheless suggest that FTY720P induces posttranslational modifications at multiple sites in the C-terminal tail of $S1P_1$.

Table 1
Phosphorylation and ubiquitination sites in the C terminus of $S1P_1$

Peptide sequence	Phosphorylation site	Ubiquitination site	Xcorr	Ascore1	Protein ID
CPSGDS#AGKFK*	S^{336}	K^{341}	1.4465	35.82	P21453
CPSGDS#AGKFK*	S^{336}	K^{341}	1.5773	35.82	P21453
CPSGDS#AGKFK*	S^{336}	K^{341}	1.4106	27.03	P21453
CPSGDS#AGKFK*	S^{336}	K^{341}	1.2418	20.91	P21453
CPSGDS#AGKFK*	S^{336}	K^{341}	1.2418	20.91	P21453
CPSGDS#AGKFK*	S^{336}	K^{341}	2.0149	27.03	P21453
RPIIAGM@EFS#R	S^{351}		1.8724		P21453
RPIIAGM@EFS#R	S^{351}		2.6827		P21453
RPIIAGM@EFS#R	S^{351}		4.2286		P21453
RPIIAGM@EFS#R	S^{351}		3.0596		P21453
RPIIAGM@EFS#R	S^{351}		2.6252		P21453
RPIIAGM@EFS#R	S^{351}		2.7061		P21453
S#K*SDNSSHPQK*	S^{353}	K^{354}, K^{363}	2.0194	5.92	P21453

Symbols within peptide sequences denote phosphorylation (#), oxidation (@), and ubiquitinylation (*). See Methods for details of Xcorr and Ascore calculations.

Phosphorylation leads to multisite polyubiquitinylation of the C-terminal tail of $S1P_1$ in the intracellular vesicles. To further analyze the importance of posttranslational modifications in the C-terminal tail of $S1P_1$, we mutated the serine residues to nonphosphorylatable alanine residues. The resulting $S1P_1$-GFP mutants were transfected into HEK293 cells, and stable clones were isolated. We then tested the ability of FTY720P to induce $S1P_1$-GFP degradation, which is completely dependent on receptor endocytosis, ubiquitinylation, and degradation (8). The S5A phosphorylation mutant (i.e., S^{351}A, S^{353}A, S^{355}A, S^{358}A, and S^{359}A) was completely resistant to FTY720P-induced degradation (Figure 2A). However, mutation of S^{336} or of 2 serines (S^{358}A and S^{359}A) did not appreciably affect FTY720P-induced receptor degradation. Mutation of 3 serines (S^{351}A, S^{353}A, and S^{355}A) partially reversed FTY720P-induced receptor degradation. These data suggest that phosphorylation of multiple serine residues is needed for FTY720P-induced $S1P_1$ degradation.

To determine the importance of ubiquitinylation of the C-terminal domain, we mutated the 4 lysine residues to non-ubiquitinatable arginines, either individually or together. As shown in Figure 2B, K^{339}R, K^{341}R, and K^{354}R mutants did not show an appreciable difference in the FTY720P-induced degradation rate. Even mutation of 2 or 3 lysines (K^{339}R and K^{341}R, or K^{339}R, K^{341}R, and K^{354}R) did not prevent FTY720P-induced degradation. In contrast, the ubiquitin acceptor mutant K4R (all 4 mutations; K^{330}R, K^{339}R, K^{341}R, and K^{354}R) completely resisted FTY720P-induced receptor degradation, which suggests that multiple ubiquitinylation events in these acceptor lysines of the C-terminal domain are required for $S1P_1$ degradation. Alternatively, ubiquitinylation at even a single lysine is sufficient to target the receptor for degradation.

To determine whether ubiquitinylation is needed for receptor endocytosis, we imaged HEK293 cells stably expressing WT ($S1P_1$-GFP), $S1P_1$-S5A-GFP, or $S1P_1$-K4R-GFP constructs by confocal fluorescence microscopy. As shown in Figure 2C, the $S1P_1$-K4R-GFP mutant exhibited receptor internalization similar to that of WT in response to S1P or FTY720P, which suggests that C-terminal ubiquitinylation is not essential for ligand-induced endocytosis. In contrast, the $S1P_1$-S5A-GFP mutant was internalization resistant, consistent with the knowledge that phosphorylation is essential for β-arrestin recruitment and receptor endocytosis (8).

We next determined the relationship between phosphorylation and ubiquitinylation in the C-terminal domain using $S1P_1$ mutants. HEK293 cells stably expressing $S1P_1$-GFP, $S1P_1$-S5A-GFP, or $S1P_1$-K4R-GFP were treated with FTY720P, and the receptor molecules were subjected to IP and IB with anti-ubiquitin antibodies. As shown in Figure 2D, the WT $S1P_1$-GFP molecule was robustly polyubiquitinylated, whereas $S1P_1$-S5A-GFP and $S1P_1$-K4R-GFP were not. These data strongly suggest that phosphorylation is required for ubiquitinylation of the C-terminal domain of $S1P_1$ after FTY720P treatment.

Identification of WWP2 as a E3 ubiquitin ligase critical for FTY720P-induced receptor degradation. We sequenced the $S1P_1$-associated polypeptides from FTY720P-treated HEK293 cells by LC/MS/MS analysis. The NEDD4 family member E3 ubiquitin ligase WWP2 (25) was identified with high statistical confidence in the proteomic analysis (Figure 3A and Table 2). To confirm the proteomic identification of WWP2, we used co-IP analysis to confirm that these 2 proteins are found in a complex. We expressed Flag-tagged $S1P_1$ and WWP2 in HEK293 cells and performed $S1P_1$ IP, followed by IB analysis with anti-WWP2 antibody. As shown in Figure 3, B and C, $S1P_1$ IPs contained WWP2, and WWP2 IPs contained $S1P_1$, which suggests that these proteins were found in a complex. The association of $S1P_1$ with WWP2 was not modulated by FTY720P treatment (Supplemental Figure 1; supplemental material available online with this article; doi:10.1172/JCI45403DS1). Interestingly, WWP2 was also found in IPs of the S5A and K4R mutants (Supplemental Figure 1), which indicates that association of this E3 ubiquitin ligase to the GPCR complex is constitutive.

Next, we determined whether WWP2 is capable of influencing the ubiquitinylation of $S1P_1$. Membrane proteins from HEK293 cells expressing WWP2 with $S1P_1$-GFP, $S1P_1$-Δ1-GFP (C-terminal deletion; ref. 9), or $S1P_1$-S5A-GFP (8) were subjected to IP with anti-GFP antibody and IB with anti-ubiquitin IgG to detect receptor ubiquitinylation. As shown in Figure 4A, polyubiquitinylation of $S1P_1$ was seen only in the WT $S1P_1$-GFP lane, which suggests that WWP2 ubiquitinylates the C-terminal domain of $S1P_1$. Additionally, since $S1P_1$-S5A-GFP was not ubiquitinylated, we conclude that phosphorylation at the C-terminal domain was required to activate the E3 ligase activity of WWP2.

We next tested the effects of WWP2 on $S1P_1$ levels in HEK293 cells in which $S1P_1$ was ectopically expressed as well as in HUVECs, which express this receptor endogenously. Overexpression of WWP2 in HEK293 cells and HUVECs resulted in enhanced degradation of $S1P_1$-GFP protein after FTY720P treatment (Figure 4, B and D). In contrast, S1P treatment did not induce degradation of the $S1P_1$-GFP protein (Supplemental Figure 2). Overexpression of related E3 ubiquitin ligases NEDD4-1, NEDD4-2, AIP4, and Cbl did not alter FTY720P-induced $S1P_1$ degradation (Supplemental Figure 3), which is suggestive of specificity. Moreover, WWP2 over expression did not induce the degradation of $S1P_1$-S5A-GFP or $S1P_1$-K4R-GFP mutants after FTY720P treatment (Supplemental Figure 4). To determine whether endogenous WWP2 is involved, we used shRNA targeted against WWP2 and prepared stable clones

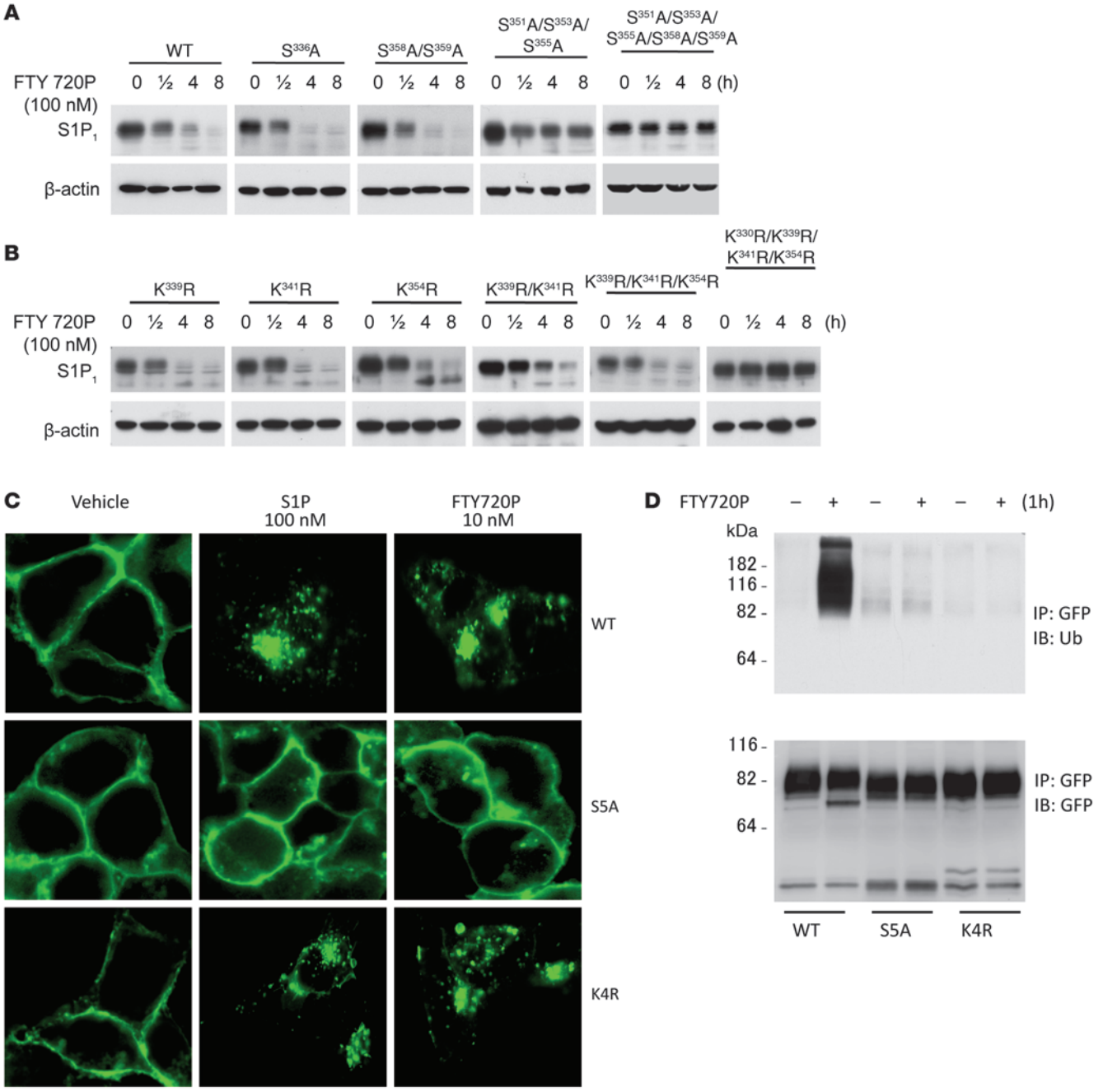

Figure 2

Phosphorylation-dependent multisite polyubiquitinylation of $S1P_1$. (**A** and **B**) $S1P_1$ WT and mutants were stably transfected into HEK293 cells and treated with 100 nM FTY720P for the indicated times, and $S1P_1$ expression was examined by IB analysis. (**C**) HEK293 cells expressing WT or degradation-resistant mutants of $S1P_1$ were treated with vehicle, S1P, or FTY720P for 1 hour and imaged with a confocal fluorescence microscope (oil immersion objective). Original magnification, ×63. (**D**) Cells in **C** were treated with 100 nM FTY720P for 1 hour, after which $S1P_1$ was subjected to IP with anti-GFP antibody and IB with anti-ubiquitin antibody.

of HEK293 cells and HUVECs by lentivirus-mediated transduction. As shown in Figure 4, C and E, substantial suppression of WWP2 polypeptide was observed concomitant with substantial attenuation of FTY720P-induced $S1P_1$ degradation in shRNA-expressing cells compared with control shRNA–expressing counterparts. These data strongly suggest that FTY720P-induced degradation of $S1P_1$ requires WWP2-dependent C-terminal ubiquitinylation of $S1P_1$.

FTY720 treatment at a supralymphopenic dose results in degradation of $S1P_1$ in vivo and induction of vascular leak. Oral administration of FTY720 to mice results in rapid and profound lymphopenia at a 0.3–0.5 mg/kg dose (7, 15, 26). We showed recently that 0.5 mg/kg FTY720 treatment induced maximal lymphopenia by 2 hours, which was sustained for more than 72 hours (7). To determine whether FTY720 induces receptor degradation in vivo,

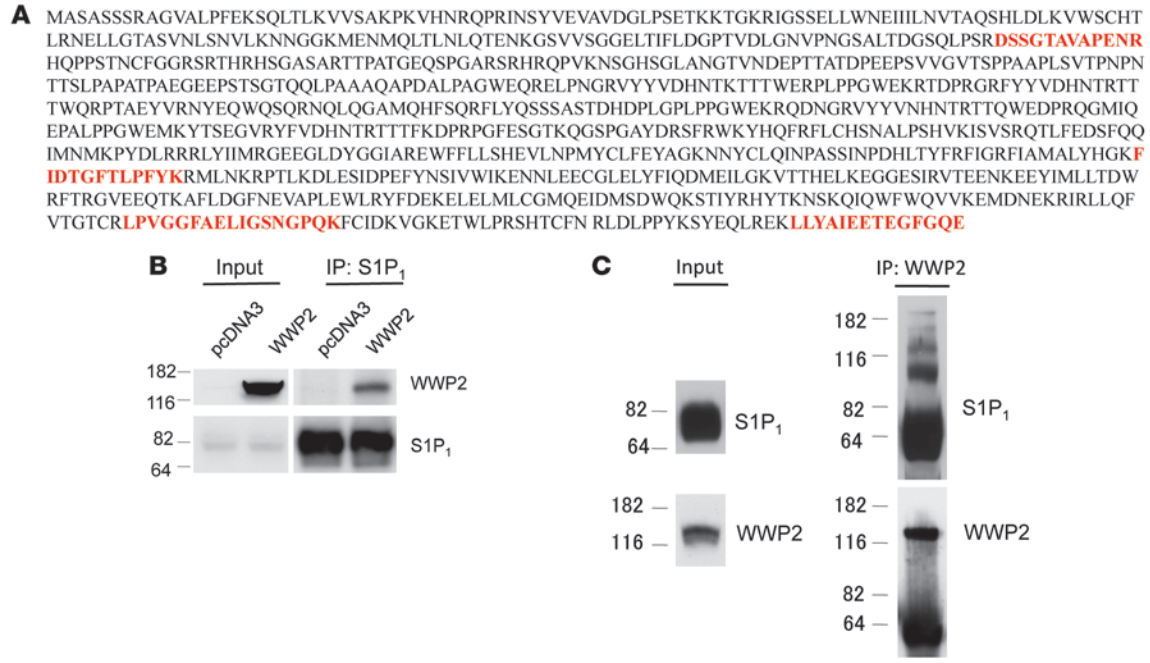

Figure 3

The E3 ubiquitin ligase WWP2 binds to $S1P_1$. (**A**) TAP of $S1P_1$ and associated polypeptides from HEK293 cells was analyzed by LC/MS/MS, which identified the NEDD4-like E3 ubiquitin-protein ligase WWP2 (accession no. O00308; locus WWP2_HUMAN; GI no. 32171765; peptide count, 4). The location of the peptides (red text) and proteomic data are shown in Table 2. (**B**) HEK293 cells expressing Flag-tagged $S1P_1$ were transiently transfected with WWP2, lysed, and subjected to IP with anti-$S1P_1$ IgG and IB with WWP2 antibody. (**C**) Cell lysates from **B** were subjected to IP by anti-WWP2 IgG and IB with $S1P_1$ antibody.

we analyzed $S1P_1$ levels in lung tissue, which abundantly expresses this receptor (27). It is also known that $S1P_1$ action is essential for adherens junction assembly (28) and inhibition of pathologic vascular permeability both in vitro (29) and in vivo (13, 30). In WT mice, a single lymphopenic dose of FTY720 (0.5 mg/kg) induced partial $S1P_1$ degradation and a measurable increase in vascular permeability. In contrast, a supratherapeutic dose (5 mg/kg) induced quantitative receptor degradation that was accompanied by a massive increase (~6-fold above basal) in vascular permeability (Figure 5, A and B).

The $S1P_1$-specific receptor modulator AUY954, a potent functional antagonist that induces receptor downregulation (31), also caused receptor degradation in the lung tissue and induced potent vascular permeability (Figure 5, C and D). In addition, W146, a competitive antagonist of $S1P_1$ (32), induced vascular permeability at early time points, even though it did not induce substantial receptor degradation. These results suggest that $S1P_1$ antagonism or degradation is responsible for increased vascular permeability in vivo.

$S1P_1$-S5A knockin mice (7) were tested to see whether defective receptor internalization affects receptor levels and vascular leak after FTY720, AUY954, or W146 treatment. As shown in Figure 5, A–D, the internalization-deficient mutant resisted receptor degradation and vascular leak markedly in response to both FTY720 and AUY954 treatment. Even though the $S1P_1$-S5A mice resisted W146-induced vascular leak, the difference was not as significant as those of the other 2 agents that induced receptor degradation. These data indicate that $S1P_1$ levels are critical for maintaining vascular integrity and resistance to vascular leak–inducing agents.

Discussion

Our work has revealed the detailed mechanism of $S1P_1$ fate after interaction with FTY720, which has entered the clinic as a disease-modifying therapy in multiple sclerosis (20, 21, 33). We showed that FTY720P potently induced a complex pattern of phosphorylation and ubiquitinylation in the C-terminal domain of $S1P_1$. Upon FTY720P treatment, C-terminal phosphorylated $S1P_1$ is endocytosed via the β-arrestin–dependent pathway (8). In this report, we documented using LC/MS/MS, multisite phosphorylation, and polyubiquitinylation of $S1P_1$. We also showed that phosphorylation was required for ubiquitinylation and that ubiquitinylation was not required for receptor endocytosis. FTY720P-induced phosphorylation and ubiquitinylation led to the proteasomal degradation of $S1P_1$. In sharp contrast, the natural ligand S1P induced internalization of $S1P_1$, but did not stimulate ubiquitinylation and degradation. The unique ability of FTY720P to induce polyubiquitinylation of $S1P_1$ may be due to its resistance to degradation by

Table 2

WWP2 peptides in $S1P_1$-associated proteins after FTY720P treatment of HEK293 cells

Position	Mass (Da)	Charge	Xcorr	dCn	Peptide
167–178	1,203.23	2+	2.4995	0.325	R.DSSGTAVAPENR.H
621–632	1,448.68	2+	3.2443	0.307	K.FIDTGFTLPFYK.R
804–820	1,683.92	2+	4.4606	0.518	R.LPVGGFAELIGSNGPQK.F
857–870	1,598.73	2+	2.5423	0.329	K.LLYAIEETEGFGQE.–

Boundaries of actual peptides identified are denoted by periods; dash after position 870 indicates the C terminus.

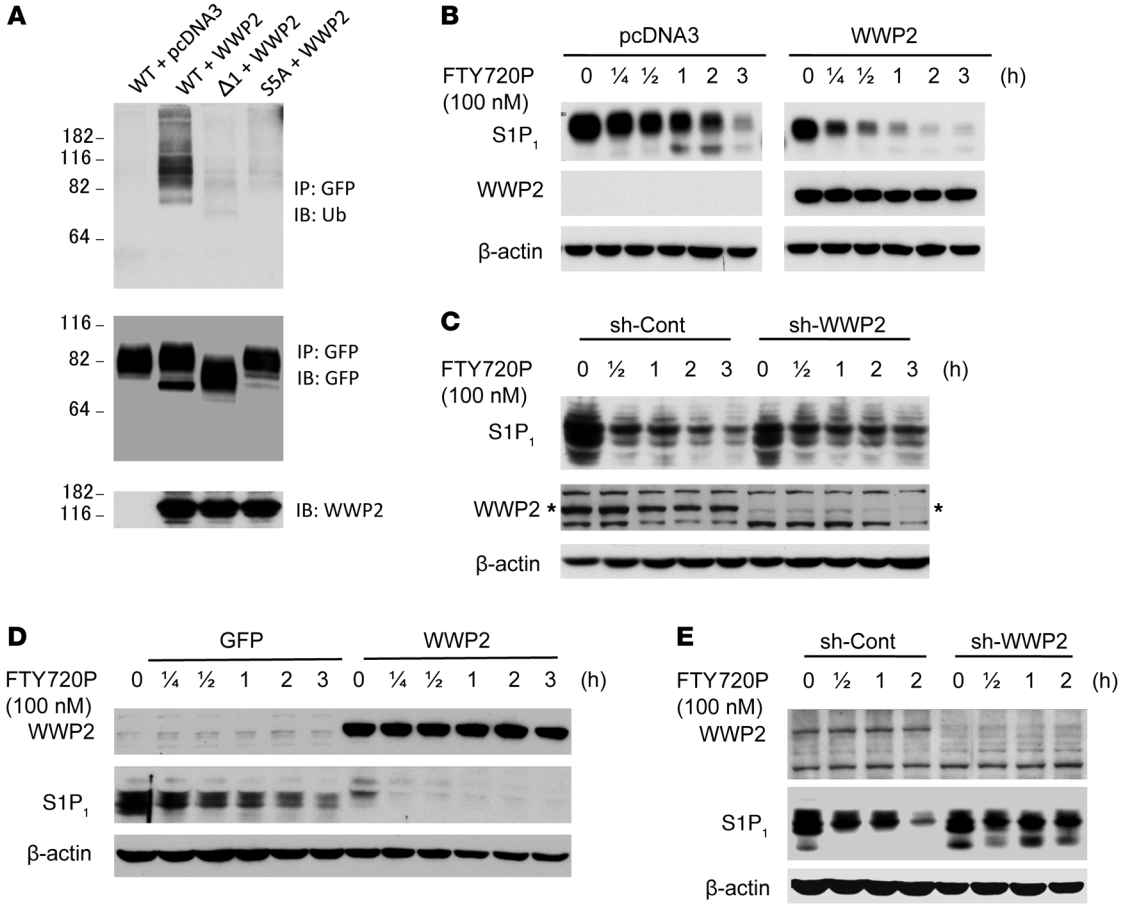

Figure 4

WWP2-dependent C-terminal polyubiquitinylation and degradation of $S1P_1$ after FTY720P treatment. (**A**) $S1P_1$-GFP, $S1P_1$-Δ1-GFP, or $S1P_1$-S5A-GFP cells were transfected with pcDNA3 or pcDNA3-WWP2, lysed, and subjected to IP with anti-GFP IgG and IB with ubiquitin antibody. The same membrane was stripped and reprobed with GFP antibody to examine receptor levels, and expression of WWP2 was determined. (**B**) Cells were treated with 100 nM FTY720P for the indicated times, and expression of $S1P_1$, WWP2, and β-actin were examined by IB analysis. (**C**) HEK293 cells expressing $S1P_1$-GFP were stably transduced with lentiviral shRNA for WWP2 (sh-WWP2) and treated with 100 nM FTY720P for the indicated times. Expression of $S1P_1$, WWP2, and β-actin were examined by IB analysis. sh-Cont, control shRNA. (**D**) HUVECs were stably transduced with lentiviral particles of pCDH-WWP2 or pCDH-copGFP and treated with 100 nM FTY720P for the indicated times, after which IB analysis was done. (**E**) Endogenous WWP2 in HUVECs was silenced by transduction of GIPZ lentiviral shRNAmir for WWP2 or control, and expression of $S1P_1$, WWP2, and β-actin was determined by IB analysis. The experiment was repeated at least 3 times with similar results.

S1P phosphatases (34) and the lyase (35). Alternatively, FTY720P-bound receptor may be locked in a conformation that prevents phosphatase action on the receptor, which may lead to blockage in receptor recycling and targeting to the degradative pathway.

Second, we identified the E3 ubiquitin ligase WWP2 by LC/MS/MS-based sequencing of $S1P_1$-associated polypeptides. Since alterations in WWP2 levels profoundly regulated the rate of FTY720P-induced $S1P_1$ degradation in HEK293 cells and HUVECs, we argue that WWP2 is a critical factor in $S1P_1$ degradation. Related E3 ubiquitin ligases NEDD4-1, NEDD4-2, AIP4, and Cbl did not alter FTY720P-induced $S1P_1$ degradation, suggestive of specificity. Interestingly, the association of $S1P_1$ with WWP2 was not modulated by FTY720P treatment. In addition, WWP2 was capable of associating with $S1P_1$-S5A and $S1P_1$-K4R mutants, which suggests that phosphorylation and ubiquitinylation of the receptor are not required. Indeed, WWP2 protein contains discrete protein interaction domains such as the WW domain and a C2 domain, which could be involved in targeting the E3 ligase to membrane domains containing $S1P_1$ (25). A similar NEDD4 family ubiquitin E3 ligase called AIP4 targets the chemokine receptor CXCR4 for degradation (36). Together, these findings suggest a model in which $S1P_1$ is found in a regulatory protein complex containing WWP2. Further activation of WWP2 likely occurs in late endosomes, where the E3 ligase activity is stimulated to catalyze polyubiquitinylation of the GPCR, leading to its proteasomal degradation. Indeed, recent findings implicate that arrestin domain–containing proteins recruit the NEDD4 E3 ligase to the endocytosed β_2-adrenergic receptor (37). Since physiological levels of S1P did not induce WWP2-dependent receptor degradation, we favor the notion that $S1P_1$ degradation by WWP2 may be a regulatory mechanism in inflammatory and immune responses when high S1P levels are produced, leading to exaggerated receptor stimulation (38), and when the pharmacological agent FTY720 is introduced. Thus, sustained internalization of $S1P_1$ would lead to WWP2-dependent $S1P_1$ degradation as a feedback regulatory mechanism.

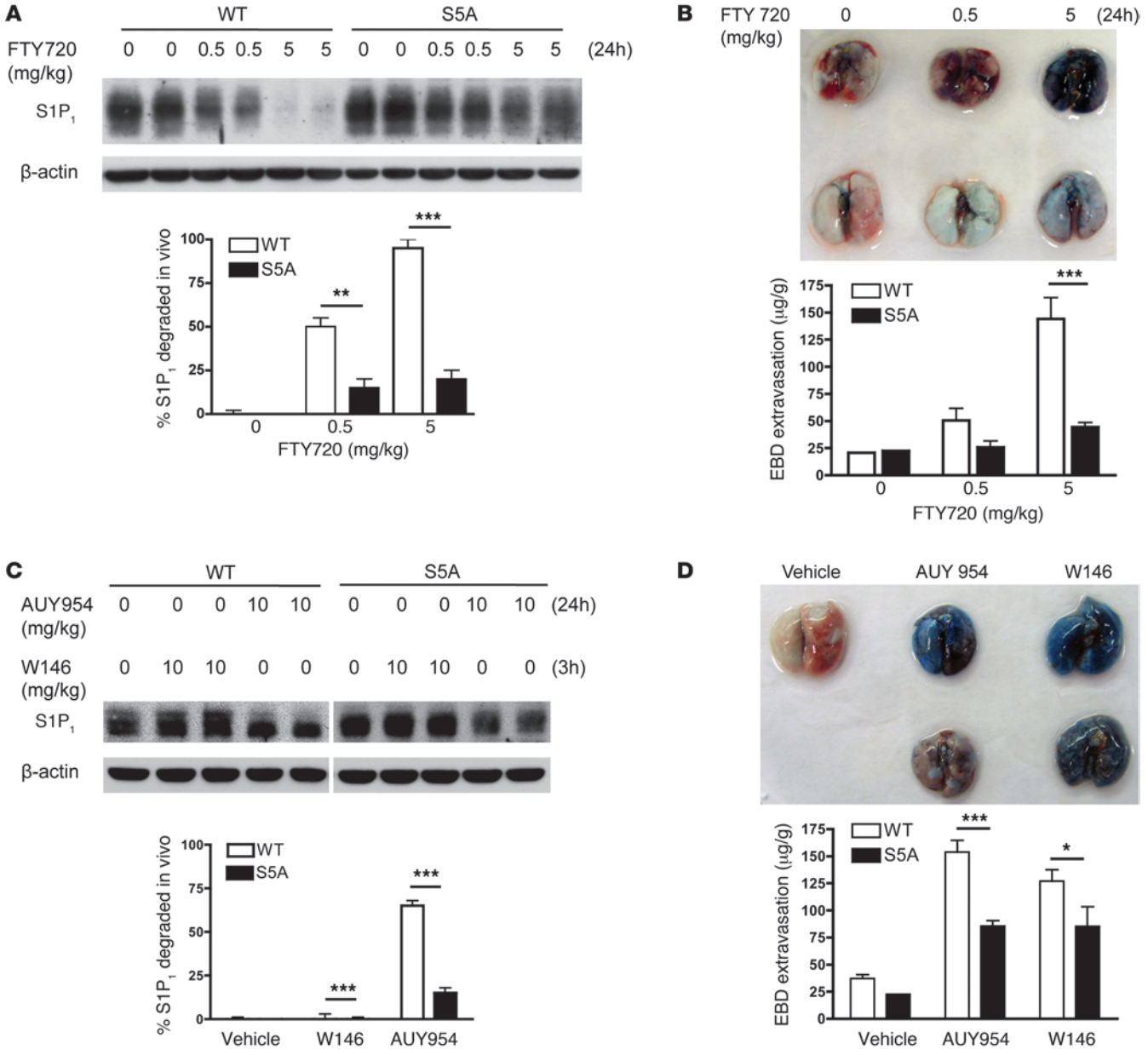

Figure 5

Degradation of $S1P_1$ in vivo induces vascular permeability. (**A**) WT and $S1P_1$-S5A knockin mice were administered FTY720 or vehicle. After 24 hours, lung membrane extracts were prepared, and $S1P_1$ antigen levels were determined. Quantification of $S1P_1$ degradation is also shown. Results are from a representative experiment repeated 3 times. $n = 3$. (**B**) FTY720 was administered to mice as in **A**. After 23 hours, EBD was intravenously injected, and lungs were photographed. To quantify vascular leak, lungs were solubilized, and EBD extravasation was determined (see Methods). $n = 17$ (WT); 7 ($S1P_1$-S5A). (**C**) WT and $S1P_1$-S5A knockin mice were administered AUY954 (10 mg/kg for 24 hours), W146 (10 mg/kg for 3 hours), or vehicle. Lung membrane extracts were prepared, and $S1P_1$ antigen levels were determined by IB analysis. Quantification of $S1P_1$ degradation is also shown. $n = 3$. (**D**) AUY954 and W146 were administered to mice as in **C**. After treatment, EBD was intravenously injected, and lungs were photographed. Lungs were then solubilized, and EBD extravasation was quantified. $n = 3$–5 (WT); 3 ($S1P_1$-S5A). All values are mean ± SD. $^*P < 0.05$; $^{**}P < 0.01$; $^{***}P < 0.001$.

Having elucidated the mechanism of $S1P_1$ degradation, we set out to understand whether this process is relevant in the efficacy or adverse events associated with FTY720 usage. Based on preclinical and clinical data, inhibition of autoreactive immune cell trafficking is thought to be the primary mode of action of FTY720 (26, 39, 40). In addition, receptor antagonism in the neural cells may also be involved in therapeutic efficacy (41). Indeed, data from mouse models demonstrate that plasma membrane–localized $S1P_1$ on immune cells determines egress rates from lymphoid organs (7, 42). Since therapeutic doses of FTY720 achieve maximal lymphopenia but only result in partial degradation of $S1P_1$, receptor degradation per se does not appear to be required for

FTY720P-induced lymphopenia. Indeed, our previous data suggest that SEW2871, which induces $S1P_1$-dependent lymphopenia (43), does not induce receptor degradation (8). Thus, lymphopenia correlates highly with receptor residency on the plasma membrane (7). In contrast, receptor degradation tracks with vascular leak.

Our present studies showed that $S1P_1$ degradation and vascular leak in the lungs of WT mice were significantly attenuated in the $S1P_1$-S5A knockin mice. We suggest that lack of C-terminal phosphorylation of vascular endothelial $S1P_1$ in the mutant mice prevents efficient internalization after FTY720 treatment and allows for sustained signaling in the plasma membrane compartment, resulting in better preservation of barrier function of the pulmonary vasculature. Although we cannot completely rule out signaling of mutant receptors in nonvascular cells or alterations in arrestin-dependent mechanisms, we favor the model of sustained plasma membrane signaling of $S1P_1$ in the preservation of EC barrier function. Moreover, our data also support the concept that internalized receptors undergo ubiquitinylation and proteasomal degradation after FTY720 treatment. AUY954, which targets $S1P_1$ selectively (31), also resulted in a similar phenomenon. Thus, reduced expression of $S1P_1$ in the vascular ECs may loosen adherens junctions (28) and induce increased vascular permeability. However, acute suppression of $S1P_1$ function by W146, a competitive $S1P_1$ selective antagonist, resulted in rapid vascular leak (30) without inducing receptor degradation. These data strongly suggest that endothelial $S1P_1$ is critical for the control of vascular permeability. This work further complements the recent finding that plasma S1P levels are required for lung endothelial barrier function (18). In addition, a recent publication demonstrated induction of vascular leak, pulmonary inflammation, and fibrosis by prolonged treatment with FTY720 and AUY954 in a bleomycin-induced mouse model (44).

Although efficacious, clinical use of FTY720 also showed dose-dependent increases in adverse events (20, 45). For example, approximately 8% of patients experienced respiratory symptoms (cough, dyspnea, bronchitis) associated with depression of lung function. In addition, approximately 5% of patients experienced macular edema. Such events are likely to be caused by increased permeability of respective vascular beds. Our data suggest that degradation of $S1P_1$ receptors induced by FTY720 may lead to increased vascular permeability. We speculate that heterogeneity in $S1P_1$ expression and/or degradation machinery may predispose some individuals to adverse effects of $S1P_1$ modulators. Since $S1P_1$ levels are under dynamic control, these findings may lead to novel strategies to upregulate vascular $S1P_1$ and obviate such side effects.

In conclusion, these studies highlight that interference with GPCR regulation can lead to mechanistically discrete steps of therapeutic modulation that can explain both efficacy and adverse events of drugs. Thus, a pharmacological agent that spares EC $S1P_1$ while targeting lymphocyte $S1P_1$ may lead to a better therapeutic index in the control of various autoimmune diseases.

Methods

Chemicals and reagents. S1P was purchased from Biomol Research Laboratories Inc. FTY720 and W146 were purchased from Cayman Chemical. AUY954 was a gift from Novartis Pharmaceuticals. Fatty acid–free BSA, β-glycerophosphate, CHAPS, and β-actin antibody were from Sigma-Aldrich. n-Octyl-β-D-glucopyranoside (OG) was from A.G. Scientific Inc. Ubiquitin monoclonal antibody (P4D1) and WWP2 polyclonal antibody were from Santa Cruz Biotechnology Inc. GFP antibodies, monoclonal and polyclonal, were from Abcam.

Cell culture and transfection. HEK293 cells stably expressing $S1P_1$ WT and various mutants tagged with GFP were grown in DMEM supplemented with 10% heat-inactivated FBS (Invitrogen), 50 U/ml penicillin, and 50 μg/ml streptomycin (Invitrogen). HUVECs (p4-10; Clonetics) were cultured in M199 medium supplemented with 10% FBS and heparin-stabilized endothelial growth factor, as previously described (46). HEK293 cells were transfected with the indicated expression plasmids using calcium phosphate–mediated transfection or LipofectAMINE 2000 transfection reagent or oligofectamine (Invitrogen) according to the manufacturer's instructions.

DNA and shRNA lentiviral constructs. GFP-tagged $S1P_1$ (WT and mutants) or $S1P_1$ WT were generated by PCR using pEGFP-N1 (EDG1) $S1P_1$ (9) as a template and inserted into pcDNA3 vector or into TAP-tagged (chitin-binding domain/calmodulin-binding domain; provided by M. Wright, University of Iowa, Carver School of Medicine, Iowa City, Iowa, USA) pcDNA3.1 vector. Human GIPZ lentiviral shRNAmir for WWP2 (clone ID, V2LHS_13525, V2LHS_196442, V2LHS_261811) and pGIPZ lentiviral shRNAmir control vector were from Thermo Scientific/Open Biosystems Inc. Production of viral particles from HEK293T was performed according to the manufacturer's instructions. The lentiviral particles were incubated with HEK293 cells stably expressing $S1P_1$-GFP and HUVECs in their growth medium. 48 hours later, all cells were selected in Puromycin (1–2 μg/ml) for 1 week. Cells were lysed and examined for WWP2 expression by Western blot and real-time quantitative RT-PCR.

For WWP2 overexpression, full-length WWP2 was transferred from pcDNA3 vector (expression plasmid provided by M. Ikeda and R. Longnecker, Northwestern University, Chicago, Illinois, USA) into lentiviral vector pCDH from System Biosciences. HEK293T cells were transfected by pCDH-WWP2 together with pPACK packaging plasmid mix. 48 hours later, lentiviral particles were collected and incubated in HUVECs. WWP2-transduced HUVECs were selected with puromycin (1–2 μg/ml) in growth media for 1 week. As a control, HUVECs were stably transduced with lentiviral particles of cop-GFP collected from cotransfection of pCDH-copGFP and pPACK packaging plasmid mix into HEK293T cells.

pRK5-AIP4, pRc/CMV-Nedd4-1, pRc/CMV-Nedd4-2, and KIAA0439 were provided by the laboratories of T. Pawson (Mount Sinai Hospital, Samuel Lunenfeld Research Institute, Toronto, Ontario, Canada) and D. Rotin (Hospital for Sick Children, Toronto, Ontario, Canada). The expression plasmid of c-Cbl was a gift from B. Mayer (University of Connecticut Health Center, Farmington, Connecticut, USA). pcDNA3.1-flag-AIP4 was provided by M. Ikeda and R. Longnecker (Northwestern University, Chicago, Illinois, USA).

Analysis of $S1P_1$ degradation by IB. HEK 293 stable clones of $S1P_1$ WT and its mutant variants were grown to 50%–65% confluence, incubated in 2% charcoal-stripped serum for 2 days and starved additional 2 hours in serum-free DMEM. Cells were then treated with FTY720P (10 nM–100 nM) for indicated times. Cells were washed with PBS and lysed by addition of SDS sample buffer, sonication briefly, denatured at 95°C for 5 minutes. Protein concentrations were determined by Pierce bicinchoninic acid (BCA) protein assay kit. Equal amounts of proteins were separated into 10% polyacrylamide gel and transblotted on nitrocellulose membrane. Blots were incubated with anti-$S1P_1$ polyclonal antibody (H60; Santa Cruz Biotechnology Inc.) and visualized by chemiluminescence (Millipore). Blots were then stripped and probed by anti–β-actin antibodies (Sigma-Aldrich). Films were scanned and normalized for total protein using the β-actin blots.

Immunofluorescence analysis. 2×10^5 cells were plated in fibronectin-coated 35-mm glass-bottom Petri dishes. 1 day later, cells were incubated in 2% charcoal-treated FBS for 2 days, washed, and serum starved 2 hours before experiment. Cells were washed with ice-cold PBS, fixed, and examined on a Zeiss LSM710 confocal microscope. For immunofluorescence analysis, $S1P_1$ (H60; Santa Cruz Biotechnology Inc.) polyclonal antibody was con-

ducted and antibody staining was visualized with Alexa Fluor 488 goat anti-rabbit for polyclonal (1:2,000 dilution) IgG (Invitrogen). Fluorescence was excited using a 488-nm argon laser, and emitted fluorescence was detected with 505-nm long-pass filter.

Detection of ubiquitinated receptors. $S1P_1$-expressing HEK293 cells in 100 mm dish (~90% confluent) were cultured with 2% charcoal-stripped serum for 2 days. Then medium was replaced by serum-free DMEM for 2 hours and incubated with FTY720P for 1 hour and lysed (50 mM Tris, pH 7.4; 150 mM NaCl; 1% Triton X-100; 10 mM β-glycerophosphate; 1 mM Na_3VO_4; 1 mM NaF; 20 mM CHAPS). Cell lysates were precleared by protein A/G agarose beads and subjected to IP with anti-GFP polyclonal antibody overnight, and $S1P_1$-bound proteins were separated in 10 % SDS-PAGE gel and probed with anti-ubiquitin antibody. For protein binding between $S1P_1$ and WWP2, cells were extracted with the lysis buffer containing 0.5% Triton X-100 and centrifuged as described above.

Analysis of $S1P_1$ expression in the mice. All animal protocols were approved by the IACUC of University of Connecticut Health Center and Weill Cornell Medical College. C57BL/6 mice were purchased from The Jackson Laboratory. Generation of the internalization-deficient *S1p1*$^{S5A/S5A}$ mice was described previously (7). Briefly, a mutant $S1P_1$ (SRSKSDNSS to ARAKADNAA) was knocked into the mouse genome by homologous recombination.

FTY720 treatment. WT and S5A-$S1P_1$ mice (6–8 weeks old) were treated by oral gavage with 0.5 or 5 mg/kg FTY720 in 2% 2-hydoxypropyl-β-cyclodextran (Sigma-Aldrich). Control animals received 2% 2-hydoxypropyl-β-cyclodextran (vehicle) in water. The mice were anesthetized by a cocktail of 100 mg/kg ketamine plus 100 mg/kg xylazine by i.p. injection. Then, the chest wall was opened to expose the heart. The left ventricle of the heart was cut, and 5 ml filtered PBS was perfused into the right ventricle through the needle of the in vivo perfusion system (AutoMate Scientific Inc.). Then heart, thymus, and lung were removed and immediately transferred into liquid nitrogen. For protein extraction from the lungs, fresh tissue was chopped, resuspended in hypotonic buffer (10 mM Tris-HCl, pH 7.8–8.0; 1 mM EDTA), blended by polytron, and placed on ice for 10–15 minutes. Lung tissue in hypotonic buffer was then homogenized by Dounce Tissue Grinder, 7 ml, 13 × 82 mm, and transferred into 1.5 ml eppendorf tubes. Tissues were further subjected to 3 freeze/thaw cycles. The homogenate was then centrifuged for 15 minutes at 32,869 *g* at 4°C. The supernatant was discarded, and the membrane pellet was washed with PBS 3 times and resuspended in 300 μl extraction buffer by repeated pipetting. Membrane proteins were then extracted by rotation in cold room for 16 hours. The lysates were centrifuged for 5 minutes at 10,000 *g* at 4°C. The supernatant was collected, and protein concentration was determined by Pierce BCA protein assay kit. $S1P_1$ protein level was then examined by Western blot.

TAP of $S1P_1$ protein for MS/MS. HEK293 cells were stably transfected by pCDNA3.1-$S1P_1$-TAP plasmid using G418 selection. $S1P_1$ protein was purified according to the TAP-tagged protein purification procedure (47, 48), with some modifications. Briefly, HEK293 cells stably expressing neomycin G418–resistant $S1P_1$ were washed twice with cold PBS and lysed in chilled buffer including 50 mM Tris-HCl (pH 8), 1 mM Na_3VO_4, 10 mM glycero-2-phosphate, 10% glycerin, 1% Triton X-100, 20 mM CHAPS, 60 mM OG, 5 mM sodium pyrophosphate, and 150 mM NaCl. Cell lysates were cleared by centrifugation at 10,000 *g* for 15 minutes and 100,000 *g* for 60 minutes again. The clear supernatants were incubated with chitin beads by rocking for overnight at 4°C. The chitin column was washed with TEV (enzyme digestion site; E*xx*Y*x*QS/G) buffer (10 mM Tris-HCl, pH 8; 0.5 mM EDTA, pH 8; 1% Triton X-100; 20 mM CHAPS; 60 mM OG; 150 mM NaCl; 1 mM DTT). TEV cleavage was performed using AcTEV protease (Invitrogen) according to the manufacturer's instructions. TEV-cleaved proteins were incubated with calmodulin beads in calmodulin-binding buffer (10 mM Tris-Cl, pH 8.0; 10 mM 2-mercaptoethanol; 150 mM NaCl; 1 mM magnesium acetate; 1 mM imidazole; 2 mM $CaCl_2$; 1% Triton X-100) overnight at 4°C. After the beads were washed with calmodulin-binding buffer, bound proteins were eluted with EGTA buffer, containing 25 mM EGTA in PBS or boiled in low SDS-PAGE sample buffer.

Sample preparation for mass spectrometry analysis of $S1P_1$ and its associated polypeptides. Affinity-purified receptor and receptor-associated proteins were separated on a 4%–12% linear gradient NuPage gel (Invitrogen). Gels were lightly stained with Coomassie blue R-250 (50% methanol, 10% acetic acid, 0.1% R-250) for 10 minutes and destained overnight in destaining solution (5% methanol, 7% acetic acid). After imaging, the area from the top to the bottom of each lane of the Coomassie-stained gel was cut essentially at 2-mm intervals (some slices were wider because of the absence of any prominent band at those positions). Each gel slice was cut into small pieces (approximately 1-mm cubes) and transferred to 500-μl microcentrifuge tubes. The gel pieces were washed with 200 μl of 50 mM NH_4HCO_3 for 30 minutes at room temperature. The supernatant was removed, and 200 μl destaining solution (50 mM NH_4HCO_3 in 50% CH_3CN) was added for 20 minutes at room temperature. The gel pieces were completely destained by repeated washes with NH_4HCO_3 and NH_4HCO_3/CH_3CN if necessary. The destained gel pieces were dehydrated with 100% CH_3CN and dried briefly in a vacuum concentrator (CentriVap). Gel pieces were rehydrated with 20–30 μl trypsin solution (12.5 ng/μl in 100 mM NH_4HCO_3) on ice for 45 minutes. In-gel digestion was performed at 37°C for 18–20 hours. The resulting peptides were extracted according to the protocol of Shevchenko et al. (49). Extracted peptides were dried in Centrivap, redissolved in solvent A (5% acetonitrile, 0.4% acetic acid, and 0.005% heptaflourobutyric acid), and stored at –20°C until mass spectrometric analysis was performed.

LC/MS/MS. To identify unmodified peptides from $S1P_1$, $S1P_1$ phosphopeptides, $S1P_1$-ubiquitinated peptides, and peptides from $S1P_1$-associated proteins, MS/MS was performed on a linear ion trap (LTQ; Thermo Finnigan) platform. A microcapillary fused silica column (12 cm long, 200 μm inside diameter) was packed with Magic C18 beads (5 μm particle size, 200-Å pore size; Michrom Bioresources). Peptides were separated at a flow rate of 200 nl/min by flow splitting. The solvent gradient of HPLC was linear from 100% solvent A (5% acetonitrile, 0.4% acetic acid, 0.005% heptafluorobutyric acid) to 80% solvent B (100% acetonitrile, 0.4% acetic acid, 0.005% heptafluorobutyric acid) for 85 minutes. The eluent was introduced directly into an LTQ mass spectrometer via electrospray ionization. Each full mass spectrometry scan was followed by 5 MS/MS scans of the most intense ions with data-dependent selection using the dynamic exclusion option (Top 5 method).

Identification of $S1P_1$-interacting proteins and posttranscriptional modification of $S1P_1$. The acquired data files were converted to .dat file format prior to searching the sequence database. MS/MS datasets were searched against a composite database of human protein sequences (56,709 entries, release November 30, 2004, downloaded from Advanced Biomedical Computation Center, NCI-Frederick; database UniProtKB/Swiss-Prot was used for searching, release 56.9 on March 3, 2009, http://www.ebi.ac.uk/uniprot/) and its reverse complement with the SEQUEST algorithm (SEQUEST-PVM, version 27, revision 0) on a multinode Linux cluster. SEQUEST parameters were as follows: all presearch filtering thresholds disregarded; mass tolerance of 3.0 Da for precursor ions; full tryptic-end constraint with allowing for 1 potential missed cleavage; variable modification (+80.0 Da) to account for potential phosphorylations on serine, threonine, and tyrosine residues; variable modification of ubiquitination (+114.1 Da) for potential ubiquitination on lysine residues; variable modification of Met (+16.0 Da). SEQUEST summary files were submitted to INTERACT (50) for subsequent data filtering. For identification of $S1P_1$-associated proteins, the dataset was filtered with following stringent X-correlation score (Xcorr) criteria: 1.8, 2.2, and 3.5 for 1+, 2+, and 3+ peptides, respectively. Under this criterion, WWP2 (NEDD4-like E3 ubiquitin-protein ligase) was identified with 4 unique peptides with high confidence. In the case of iden-

tification of $S1P_1$ phosphorylation and ubiquitination sites, Xcorr was less stringent: 1.6, 1.8, and 3.0 for 1+, 2+, and 3+ peptides, respectively. In all cases, delta correlation score (dCn) was 0.1 or greater. To measure the probability of correct phosphorylation site localization (Ascore calculation, $-10\log_P$; ref. 51), the phosphopeptide dataset was submitted to http://ascore.med.harvard.edu/ascore.php. Finally, all potential MS/MS spectral matches were subjected to manual inspection as a final validation step prior to acceptance as valid peptide identification. The spectral count of identified phosphopeptides and ubiquitinated peptides from FTY720P-treated or untreated samples was used for qualitative measurement of $S1P_1$-mediated events.

Lung permeability assay. Pulmonary vascular leakage after administration of FTY720, AUY954, or W146 was measured by Evan blue dye (EBD) accumulation assay. EBD (0.5% in saline) was injected into the tail vein for 90 minutes before tissue harvest. FTY720 (oral gavage) and AUY954 (i.p.) were treated for 24 hours, whereas W146 was treated for 3 hours. Pulmonary vasculature was perfused with 5 ml normal saline through the right ventricle, while allowing the perfusate to drain from the incision in the left ventricle. Lungs were removed, photographed, weighed, and dried at 56°C overnight. Dry lung weight was measured again, and EBD was dissolved in formamide (Sigma-Aldrich) at 37°C for 24 hours and quantitated spectrophotometrically at 620 and 740 nm.

Statistics. Statistical analysis for all experiments was performed using 2-way ANOVA followed by Bonferroni post-tests for group comparison using Prism software. A P value less than 0.05 was considered significant.

Acknowledgments

This work was supported by NIH grants HL89934 and HL70694 to T. Hla and by an AHA Founders affiliate postdoctoral fellowship award to M.L. Oo. We thank Michael Wright, Masato Ikeda, Richard Longnecker, Tony Pawson, Bruce Mayer, and Daniela Rotin for the gift of reagents and Ralph Nachman, Domenic Falcone, Andrew J. Dannenberg, and Hideru Obinata for critical comments.

Received for publication October 12, 2010, and accepted in revised form March 30, 2011.

Address correspondence to: Timothy Hla, Department of Pathology and Laboratory Medicine, Center for Vascular Biology, Box 69, Weill Cornell Medical College, Cornell University, 1300 York Avenue, New York, New York 10065, USA. Phone: 212.746.9953; Fax: 212.746.2830; E-mail: tih2002@med.cornell.edu.

1. Hannun YA, Obeid LM. Principles of bioactive lipid signalling: lessons from sphingolipids. *Nat Rev Mol Cell Biol*. 2008;9(2):139–150.
2. Hla T, Lee MJ, Ancellin N, Paik JH, Kluk MJ. Lysophospholipids--receptor revelations. *Science*. 2001;294(5548):1875–1878.
3. Schwab SR, Pereira JP, Matloubian M, Xu Y, Huang Y, Cyster JG. Lymphocyte sequestration through S1P lyase inhibition and disruption of S1P gradients. *Science*. 2005;309(5741):1735–1739.
4. Hla T, Venkataraman K, Michaud J. The vascular S1P gradient-cellular sources and biological significance. *Biochim Biophys Acta*. 2008;1781(9):477–482.
5. Lee MJ, et al. Sphingosine-1-phosphate as a ligand for the G protein-coupled receptor EDG-1. *Science*. 1998;279(5356):1552–1555.
6. Matloubian M, et al. Lymphocyte egress from thymus and peripheral lymphoid organs is dependent on S1P receptor 1. *Nature*. 2004;427(6972):355–360.
7. Thangada S, et al. Cell-surface residence of sphingosine 1-phosphate receptor 1 on lymphocytes determines lymphocyte egress kinetics. *J Exp Med*. 2010;207(7):1475–1483.
8. Oo ML, et al. Immunosuppressive and anti-angiogenic sphingosine 1-phosphate receptor-1 agonists induce ubiquitinylation and proteasomal degradation of the receptor. *J Biol Chem*. 2007;282(12):9082–9089.
9. Liu CH, Thangada S, Lee MJ, Van Brocklyn JR, Spiegel S, Hla T. Ligand-induced trafficking of the sphingosine-1-phosphate receptor EDG-1. *Mol Biol Cell*. 1999;10(4):1179–1190.
10. Bankovich AJ, Shiow LR, Cyster JG. CD69 suppresses sphingosine 1-phosophate receptor-1 (S1P1) function through interaction with membrane helix 4. *J Biol Chem*. 2010;285(29):22328–22337.
11. Shiow LR, et al. CD69 acts downstream of interferon-alpha/beta to inhibit S1P1 and lymphocyte egress from lymphoid organs. *Nature*. 2006;440(7083):540–544.
12. Billich A, Bornancin F, Devay P, Mechtcheriakova D, Urtz N, Baumruker T. Phosphorylation of the immunomodulatory drug FTY720 by sphingosine kinases. *J Biol Chem*. 2003;278(48):47408–47415.
13. Sanchez T, et al. Phosphorylation and action of the immunomodulator FTY720 inhibits vascular endothelial cell growth factor-induced vascular permeability. *J Biol Chem*. 2003;278(47):47281–47290.
14. Brinkmann V, et al. The immune modulator FTY720 targets sphingosine 1-phosphate receptors. *J Biol Chem*. 2002;277(24):21453–21457.
15. Mandala S, et al. Alteration of lymphocyte trafficking by sphingosine-1-phosphate receptor agonists. *Science*. 2002;296(5566):346–349.
16. Graler MH, Goetzl EJ. The immunosuppressant FTY720 down-regulates sphingosine 1-phosphate G protein-coupled receptors. *FASEB J*. 2004;18(3):551–553.
17. Pham TH, Okada T, Matloubian M, Lo CG, Cyster JG. S1P1 receptor signaling overrides retention mediated by G alpha i-coupled receptors to promote T cell egress. *Immunity*. 2008;28(1):122–133.
18. Camerer E, et al. Sphingosine-1-phosphate in the plasma compartment regulates basal and inflammation-induced vascular leak in mice. *J Clin Invest*. 2009;119(7):1871–1879.
19. LaMontagne K, et al. Antagonism of sphingosine-1-phosphate receptors by FTY720 inhibits angiogenesis and tumor vascularization. *Cancer Res*. 2006;66(1):221–231.
20. Cohen JA, et al. Oral fingolimod or intramuscular interferon for relapsing multiple sclerosis. *N Engl J Med*. 2010;362(5):402–415.
21. Kappos L, et al. A placebo-controlled trial of oral fingolimod in relapsing multiple sclerosis. *N Engl J Med*. 2010;362(5):387–401.
22. Aktas O, Kury P, Kieseier B, Hartung HP. Fingolimod is a potential novel therapy for multiple sclerosis. *Nat Rev Neurol*. 2010;6(7):373–382.
23. Brinkmann V, et al. Fingolimod (FTY720): discovery and development of an oral drug to treat multiple sclerosis. *Nat Rev Drug Discov*. 2010;9(11):883–897.
24. Tsai A, Carstens RP. An optimized protocol for protein purification in cultured mammalian cells using a tandem affinity purification approach. *Nat Protoc*. 2006;1(6):2820–2827.
25. McDonald FJ, Western AH, McNeil JD, Thomas BC, Olson DR, Snyder PM. Ubiquitin-protein ligase WWP2 binds to and downregulates the epithelial Na(+) channel. *Am J Physiol Renal Physiol*. 2002;283(3):F431–F436.
26. Brinkmann V. FTY720 (fingolimod) in Multiple Sclerosis: therapeutic effects in the immune and the central nervous system. *Br J Pharmacol*. 2009;158(5):1173–1182.
27. Chae SS, Proia RL, Hla T. Constitutive expression of the S1P1 receptor in adult tissues. *Prostaglandins Other Lipid Mediat*. 2004;73(1–2):141–150.
28. Lee MJ, et al. Vascular endothelial cell adherens junction assembly and morphogenesis induced by sphingosine-1-phosphate. *Cell*. 1999;99(3):301–312.
29. Garcia JG, et al. Sphingosine 1-phosphate promotes endothelial cell barrier integrity by Edg-dependent cytoskeletal rearrangement. *J Clin Invest*. 2001;108(5):689–701.
30. Sanna MG, et al. Enhancement of capillary leakage and restoration of lymphocyte egress by a chiral S1P1 antagonist in vivo. *Nat Chem Biol*. 2006;2(8):434–441.
31. Pan S, et al. A monoselective sphingosine-1-phosphate receptor-1 agonist prevents allograft rejection in a stringent rat heart transplantation model. *Chem Biol*. 2006;13(11):1227–1234.
32. Gonzalez-Cabrera PJ, et al. Full pharmacological efficacy of a novel S1P1 agonist that does not require S1P-like headgroup interactions. *Mol Pharmacol*. 2008;74(5):1308–1318.
33. Massberg S, von Andrian UH. Fingolimod and sphingosine-1-phosphate--modifiers of lymphocyte migration. *N Engl J Med*. 2006;355(11):1088–1091.
34. Mechtcheriakova D, et al. FTY720-phosphate is dephosphorylated by lipid phosphate phosphatase 3. *FEBS Lett*. 2007;581(16):3063–3068.
35. Bandhuvula P, Tam YY, Oskouian B, Saba JD. The immune modulator FTY720 inhibits sphingosine-1-phosphate lyase activity. *J Biol Chem*. 2005;280(40):33697–33700.
36. Marchese A, Raiborg C, Santini F, Keen JH, Stenmark H, Benovic JL. The E3 ubiquitin ligase AIP4 mediates ubiquitination and sorting of the G protein-coupled receptor CXCR4. *Dev Cell*. 2003;5(5):709–722.
37. Nabhan JF, Pan H, Lu Q. Arrestin domain-containing protein 3 recruits the NEDD4 E3 ligase to mediate ubiquitination of the beta2-adrenergic receptor. *EMBO Rep*. 2010;11(8):605–611.
38. Massberg S, et al. Immunosurveillance by hematopoietic progenitor cells trafficking through blood, lymph, and peripheral tissues. *Cell*. 2007;131(5):994–1008.
39. Mehling M, et al. FTY720 therapy exerts differential effects on T cell subsets in multiple sclerosis. *Neurology*. 2008;71(16):1261–1267.
40. Mehling M, et al. Th17 central memory T cells are reduced by FTY720 in patients with multiple sclerosis. *Neurology*. 2010;75(5):403–410.
41. Choi JW, et al. FTY720 (fingolimod) efficacy in an animal model of multiple sclerosis requires astrocyte sphingosine 1-phosphate receptor 1 (S1P1) modulation. *Proc Natl Acad Sci U S A*. 2011;108(2):751–756.

42. Schwab SR, Cyster JG. Finding a way out: lymphocyte egress from lymphoid organs. *Nat Immunol*. 2007;8(12):1295–1301.
43. Jo E, et al. S1P1-selective in vivo-active agonists from high-throughput screening: off-the-shelf chemical probes of receptor interactions, signaling, and fate. *Chem Biol*. 2005;12(6):703–715.
44. Shea BS, Brooks SF, Fontaine BA, Chun J, Luster AD, Tager AM. Prolonged exposure to sphingosine 1-phosphate receptor-1 agonists exacerbates vascular leak, fibrosis, and mortality after lung injury. *Am J Respir Cell Mol Biol*. 2010;43(6):662–673.
45. Kappos L, et al. Oral fingolimod (FTY720) for relapsing multiple sclerosis. *N Engl J Med*. 2006; 355(11):1124–1140.
46. Hla T, Maciag T. An abundant transcript induced in differentiating human endothelial cells encodes a polypeptide with structural similarities to G-protein-coupled receptors. *J Biol Chem*. 1990;265(16):9308–9313.
47. Rigaut G, Shevchenko A, Rutz B, Wilm M, Mann M, Seraphin B. A generic protein purification method for protein complex characterization and proteome exploration. *Nat Biotechnol*. 1999; 17(10):1030–1032.
48. Puig O, et al. The tandem affinity purification (TAP) method: a general procedure of protein complex purification. *Methods*. 2001;24(3):218–229.
49. Shevchenko A, Wilm M, Vorm O, Mann M. Mass spectrometric sequencing of proteins silver-stained polyacrylamide gels. *Anal Chem*. 1996;68(5):850–858.
50. Han DK, Eng J, Zhou H, Aebersold R. Quantitative profiling of differentiation-induced microsomal proteins using isotope-coded affinity tags and mass spectrometry. *Nat Biotechnol*. 2001;19(10):946–951.
51. Beausoleil SA, Villén J, Gerber SA, Rush J, Gygi SP. A probability-based approach for high-throughput protein phosphorylation analysis and site localization. *Nat Biotechnol*. 2006;24(10):1285–1292.